J Therm Anal Calorim
DOI 10.1007/s10973-015-4496-1

Thermal characterization of a new green ceramic material by heating microscopy, thermogravimetry and differential thermal analysis

Brites Fontoura Rangel · Marcelo Mendes Viana · Marcus Vinícius A. Fonseca · Jo Dweck · Luís Marcelo Tavares

Received: 23 September 2014 / Accepted: 25 January 2015

Abstract A new ceramic material "Vikaflex®" was developed from industrially pyrolized shale solid residue. Thermal properties of this material were studied by thermal microscopy, TG, DTG and DTA analyses at temperature from 400 to 1,400 °C. The thermal expansion coefficient was estimated from the heating microscope images for the solid phase before losing its shape using an improvement of a previous method. The specific heat capacity and mass change between 600 and 1,100 °C were detected. This porous solid material shows high thermal stability up to 1,050 °C.

Keywords Ceramic · Glass · Residue from shale · Foam · Thermogravimetry · Expansion coefficient

Introduction

Industrial activities are permanently pressed toward reducing production costs, improving quality of products and innovating through new processes and materials in order to maintain a sustainable production. The direct environmental impact resulting from the increase in the generation of residues associated with these industrial activities, as well as the high costs associated with their disposal, has been motivating the development of new processes to immobilize and reuse these residues. Such developments are well aligned with the premises of Agenda 21 document, which deals with the reduction in industrial environment liabilities [1–3].

Different ceramic materials have been developed from the thermal processing of shale. For instance, porous sintered blocks, made from a number of miscellaneous wastes, including shale powder, were used for building and construction [4–6]. Shale was used as a raw material in the production of red fired ceramics at 1,100 °C [7], while various combinations of shales and clays have been used to manufacture ceramic tiles and bricks, in which shales corresponded to the non-plastic component [8].

Glasses have also been developed from shale [3]. Residues of shale processing were the main raw material in the preparation of sintered ceramic foams and glass-ceramics foams with insulating properties [9–12]. A bubbled glass was manufactured by firing a mold filled with powders of foamable and expandable shale as building construction material [13]. A light wall material, formed by vitreous foam ceramic composed of shale and other inorganic materials, was manufactured by sintering followed by cutting the resulting pieces down to the required size [14].

Shale has also been used in the manufacture of other ceramic products, such as thermal insulation sound absorption boards [15], suspended ceramic filtering materials [16], "green" low-cost two-layer wallboard products with social benefits [17] and "green" ceramic bricks as water-permeable brick billets [18].

Important researches have been carried out in Brazil, aiming at the characterization and use of wastes from oil

B. F. Rangel (✉) · L. M. Tavares
Department of Metallurgical and Materials Engineering, Universidade Federal do Rio de Janeiro – COPPE/UFRJ, Cx. Postal 68505, Rio de Janeiro, RJ CEP 21941-972, Brazil
e-mail: britesfontoura@gmail.com

M. M. Viana · J. Dweck
Thermal Analysis Laboratory, School of Chemical Engineering, TBPq, Universidade Federal do Rio de Janeiro, Rio de Janeiro, RJ, Brazil

M. V. A. Fonseca
Department of Production Engineering, Universidade Federal do Rio de Janeiro – COPPE/UFRJ, Rio de Janeiro, RJ, Brazil

Published online: 01 March 2015

shale processing, so as to reduce the volume that is disposed to the environment. Glasses and ceramic foams with low production costs and/or advanced properties have been obtained, including lightweight new products that can be useful in building, as well as the production of glasses and glass-ceramics [2, 3, 19–23].

Vikaflex® is one of these products, differentiated by being produced exclusively from industrial pyrolyzed shale residue [2]. It is a ceramic foam produced by specific treatment applied to pyroexpansible clays present in pyrolyzed shale residue. The material is molded and fired in order to take advantage, in a controlled way, of its natural expansibility [2]. Pyroexpanded clays are already commercialized as expanded clays, which are used in hydroponic production and landscaping, as finishing materials or substrates, as well as in lightweight aggregates in concrete and in manufacturing of aged stonewashed jeans. It is important to note that this kind of product does not require strict dimensional control, since they just take advantage of uncontrolled swelling characteristics of the material during its firing [2]. However, the process that is adopted to obtain Vikaflex® from these residues uses special conditions for a controlled pyroexpansion, developing important product characteristics and allowing the control of shape of the final product. The result is a light, porous, impermeable ceramic material that has thermal and acoustic insulation properties. It can be produced as ready-to-use pieces in various shapes and sizes, with innovative features in the field of ceramic foams [2].

The present paper aims to evaluate selected thermal properties of Vikaflex® by thermogravimetry and differential scanning calorimetry as well as to identify the main morphological transformations through the use of heating microscopy (HM) when this ceramic material is heated from room temperature up to melting. As a new ceramic material, Vikaflex does not yet have any data published in the literature. As such, thermogravimetry is used to evaluate the possible mass changes that are occurring as a function of temperature, due to chemical or physical transformations with mass change, such as dehydration, dehydroxylation, volatilization, adsorption, desorption, oxidation, combustion and/or decomposition. The thermogravimetric derivative curve (DTG) is used to better determinate the temperature ranges of the transformations with mass changes from respective peaks. Differential scanning calorimetry is used to identify the main thermal effects of the transformations that occur in the studied temperature range, including phase changes that are not accompanied by mass changes. In this work, the images generated by heating microscopy were used to indicate the characteristic points of shape and phase changes that are promoted by chemical and physical transformations. Additionally, these images were used to estimate quantitatively the dimensional variations of the samples and thus the linear thermal expansion coefficient during heating using a new method, which is an improvement of the one used previously by Dweck et al. [24].

Materials and methods

Materials

Vikaflex® is a ceramic foam manufactured from the residue of oil shale industrial pyrolysis in Usina de São Mateus do Sul, State of Paraná, Brazil. The residual pyrolyzed shale is pulverized, molded and sintered at about 1,100 °C, in the desired dimensions and shapes. Foaming is generated by characteristic pyroexpansion of the residue when heated up to this temperature.

The Vikaflex® samples analyzed in this work were cut from 5 × 5 × 1 cm pieces. For heating microscopy and thermal analysis runs, samples were cut in the shape of a cube with approximately 2 mm of width. The glass obtained during its thermal analysis at temperatures of up to 1,400 °C was analyzed as formed, after total melting of the original cube in the alumina crucible used for the analysis.

In order to establish a comparison between Vikaflex® and other materials, results from heating microscopy analysis were also presented for selected geological and ceramic materials used in ceramic processing. Phonolite (Chapada dos Índios, Brazil) and granite (Jundiaí, Brazil) samples were investigated previously for application as fluxes in ceramic masses [25], whereas alkaline glass samples VM-1, VM-2 and VM-3 were used for immobilization and reuse of mining residues [26].

Chemical and mineralogical composition

X-ray fluorescence analysis was performed in an EDX-720 equipment under vacuum, and x-ray diffraction data were obtained in a Shimadzu XRD-6000 equipment, using Kα radiation (30 kV, 30 mA), with a goniometer scanning velocity of 2° min^{-1}, from $2\theta = 10°$ to 80°.

Heating microscopy

Heating microscopy analysis (HM) was performed using a Leitz Wetzlar heating microscope coupled to a video camera (Samsung SDC 415 ND model). Image acquisition was carried out using a microprocessed interface Captura Frames 1.5, developed at the Electronic Computing Center (NCE) of Universidade Federal do Rio de Janeiro (UFRJ). Images of the samples under analysis

were automatically obtained and saved in real time at a frequency of 6 frames per minute, for image analysis that was carried out afterward and that allowed identifying phase and morphological changes and their corresponding temperatures. Samples were heated in still air at 10 °C min^{-1} heating rate. Besides assisting in the identification of points that are characteristic of ceramic materials, it was also possible to estimate specimen dimensional variations during heating without any external stress applied to the sample, even after the softening step, whenever required [27–30].

In the present work, because of the irregular shape of the samples, the dimensional change measurements were performed using an image analysis software (Image J) that was used in measuring the area of the cross-visible section of the sample at every 50 °C of temperature change [24]. Prior to measurements, the software was used to improve identification of the silhouette of the sample through image segmentation (Fig. 1).

The use of heating microscopy for measuring dimensional changes of Vikaflex® in the present work instead of dilatometry, the most commonly used technique, is justified on the basis of some of the following arguments:

- The application of dilatometry becomes unfeasible at temperatures above the point in which a liquid phase is formed. As will be demonstrated in the present work, this is the case of Vikaflex®, which generates a liquid phase from temperatures as low as about 900 °C.
- The visible image by HM of the tested sample consists of the shadow bounded by faces perpendicular to the camera lens, which include extreme points of these faces. As such, any possible measurement error due to the irregularity of the faces also occurs in conventional dilatometry, where the face available for measurement has always its extreme points in contact with the displacement measuring rod.

Thermal expansion coefficient

The thermal expansion coefficient was estimated from the heating microscopy (HM) images. In each image, a square grid is visible, in which three continuous square sides correspond to 1 mm. From this and the image analysis software, it was possible to estimate the cross-sectional area A of the specimen at any chosen temperature, from an initial measurement in pixels and then transforming it in mm^2.

Given the aim to estimate the coefficient of linear thermal expansion as a function of temperature, it was first necessary to transform the measured areas in equivalent linear dimensions of a regular geometric shape. In general, the diameter of an equivalent circle is estimated in these cases. In the present work, however, as the shape of the sample described by the captured images approaches a square, the length of the side of a square with the same area as that of the projected image was calculated, given by

$$L = \sqrt{A} \tag{1}$$

where A is the measured area and L is the equivalent square side at a given temperature.

Plotting L as a function of T, the least squares best fit polynomial equation was obtained, resulting in the mathematical function $L(T)$. From this equation and for the temperature range of interest, the coefficient of linear thermal expansion α at a temperature T was estimated by

$$\alpha = (\mathrm{d}L/\mathrm{d}T) / L \tag{2}$$

where $\mathrm{d}L/\mathrm{d}T$ is the derivative of the polynomial function $L(T)$.

As such, the new method used for measuring dimensional change is an improvement of that used previously by part of the authors [26], since it actually accounts for changes in all directions of specimens with irregular shapes.

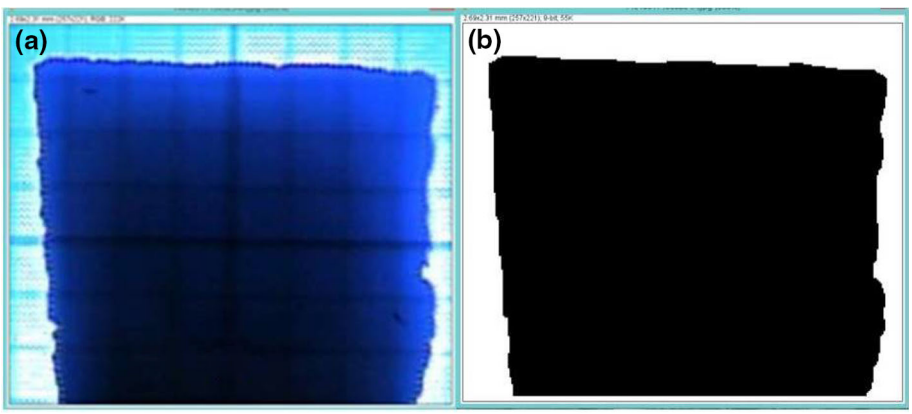

Fig. 1 Original image from heating microscopy (**a**) and image after segmentation and ready for area measurement (**b**)

Optical microscopy

Optical microscopy images, both of external and of internal (cut) surfaces of Vikaflex® pieces, were collected at room temperature using an Olympus SZH10 microscope, being captured using a Canon PowerShot SD1200 IS Digital ELPH camera. They were then later used to analyze the morphology and the porous structure of the material.

Thermal analysis

Thermal analyses (TA) of Vikaflex® and of the glass obtained after its melting were performed in a TA Instruments simultaneous TG/DSC equipment, model SDT-Q600. The analyses were performed using α-Alumina crucibles, 100 mL min^{-1} of air as purge gas, at 10 °C min^{-1} heating rate. This technique has been used to assist in explaining results obtained using the heating microscopy technique.

Results and discussion

Chemical and mineralogical composition

The composition of Vikaflex® determined by X-ray Fluorescence was 50.37 % SiO_2, 31.23 % Fe_2O_3, 13.36 % Al_2O_3, 2.49 % K_2O, 1.62 % CaO, 0.47 % SO_3 and 0.31 % ZrO_2.

The X-ray diffraction pattern is presented in Fig. 2. This, along with the Rietveld method, allowed to estimate the composition, in mass basis, of the crystalline mineral components as 51.7 % of Quartz (SiO_2), 24.6 % of Hematite (Fe_2O_3), 16.0 % of Anorthite ($CaO{\cdot}Al_2O_3{\cdot}4SiO_2$) and 7.65 % of Mullite ($3Al_2O_3{\cdot}2SiO_2$), besides a vitreous phase.

Heating microscopy

Figure 3 shows some of the morphological and phase changes of Vikaflex® between 400 and 1,400 °C obtained by heating microscopy [31–37]. Images of other characteristic sample transformation points are also shown, where:

- Figure 3a,b and c shows images of the sample at temperatures in which there are no shape changes, with expansion occurring from 450 to 900 °C and shrinkage between 900 and 1,050 °C, more noticeable under accurate analysis of an image software or expanded image view. The area measurement was considered only at temperatures of up to 1,050 °C.
- Figure 3d illustrates intermediate conditions of shape change between deformation and softening points at about 1,150 °C.
- Figure 3e shows the DIN 51730 softening point with visible anisotropic expansion at 1,200 °C.
- Figure 3f shows the DIN 51730 sphere point with significant and maximum swelling at 1,250 °C.
- Figure 3g illustrates the DIN 51730 half sphere point at 1,285 °C.
- Figure 3h illustrates the DIN 51730 total melting point at 1,400 °C.

Table 1 summarizes values of characteristic temperatures of shape and phase changes of Vikaflex®, comparing them with values for other geological and ceramic materials. It is evident that the values of the temperatures for the characteristic points of the different materials used in the manufacture of ceramic products vary significantly according to their composition. Indeed, it is known that these vary significantly with composition and production conditions, such as particle size distribution of the raw

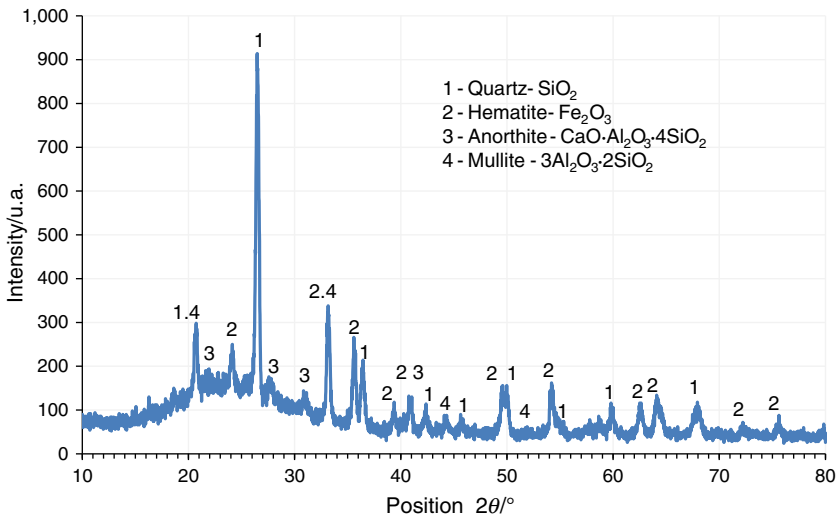

Fig. 2 Vikaflex XRD pattern

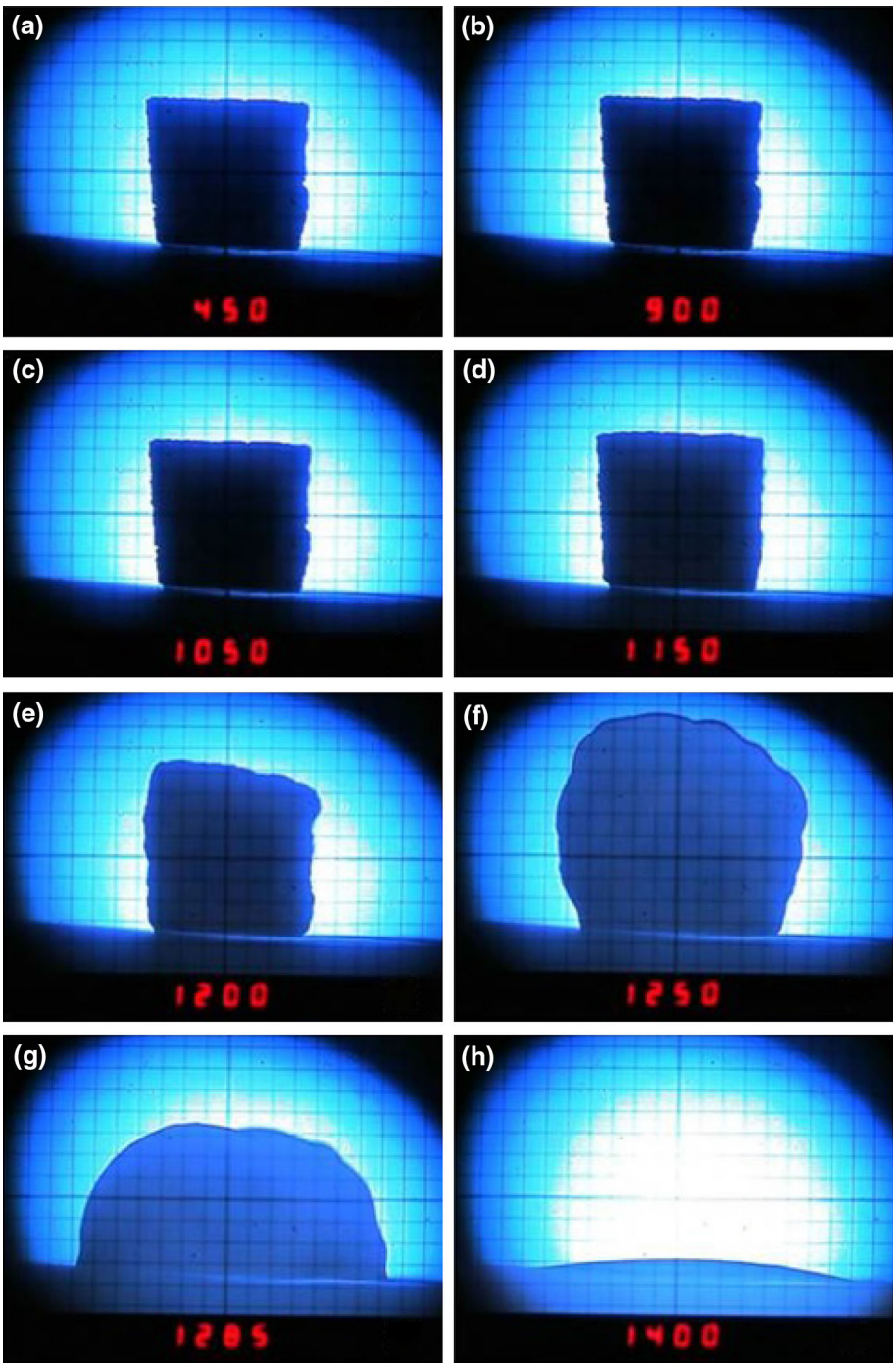

Fig. 3 Images by heating microscopy of sample T5 of Vikaflex® obtained at different temperatures (in °C), indicating specific *shape* or *phase* changes

materials, method of forming and heat treatment that is used [38, 39]. For instance, the alkaline glasses have a low softening point temperature as required for a low-cost conformation. Phonolite and granite were tested as fluxes for the ceramic industry, and phonolite was chosen as the most suitable for this role because of its lower softening temperature [25]. Table 1 shows that Vikaflex® and the ceramic flux Chapada dos Índios phonolite present characteristic points at similar temperatures and that these temperatures are not distant from the average of the characteristic temperatures of the three alkali glass [25, 26]. The Vikaflex® showed high thermal stability, resisting high temperatures, suggesting its potential use in living spaces. On the other hand, it requires processing temperatures that are compatible with those of other traditional ceramics, keeping manufacturing costs at a competitive level.

Table 1 Characteristic transformation points of selected materials and Vikaflex®

	Temperature of characteristic points/°C					
	Vikaflex®	Chapada dos Índios phonolite	Jundiaí granite	VM-1 Alkaline glass	VM-2 Alkaline glass	VM-3 Alkaline glass
Softening point	1,200	1,180	1,400	1,031	1,160	1,222
Sphere point	1,250	1,240	1,490	1,174	1,330	1,235
Half sphere point	1,285	1,280	1,560	1,179	1,400	1,425
Total melting point	1,400	1,340	1,620	1,300	1,433	1,500
Reference	This work	[25]	[25]	[26]	[26]	[26]

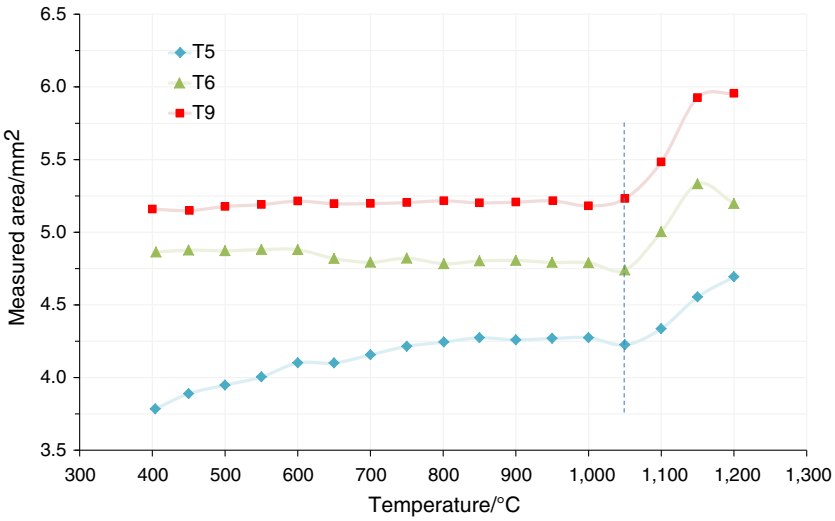

Fig. 4 Cross-sectional area of three samples of Vikaflex as a function of temperature up to 1,200 °C, showing the upper limit of 1,050 °C for the calculation of the thermal expansion coefficient

Thermal expansion coefficient

Although the area of the shadow of the samples has being measured up to 1,200 °C, only values below 1,050 °C were used for the determination of the thermal expansion coefficient, because up to this temperature, the shape of the measured areas was unchanged, as shown in Fig. 3. This indicates that up to this temperature, the material is isotropic. Above this temperature, which is called deformation temperature [33], the exposed surfaces begin to become smooth, due to the beginning of formation of a liquid phase on it.

Figure 4 presents the measurement results for samples T5, T6 and T9. The difference in the initial areas of the samples explains, at least in part, difference encountered between the three curves. The measurement was interrupted at 1,200 °C due to the abrupt expansion and deformation of the sample that occurred above approximately 1,150 °C. At this temperature, the proportion of the liquid phase increases and the viscosity of the vitreous thin layer covering the sample decreases. As the temperature increases, the greater the expansion of the sample promoted by the higher pressure of the formed gases, the easier it becomes for the gases to overcome the resistance of the thinner external glassy film and escape suddenly to the outside environment, causing sudden volume shrinkage. This effect appears intermittently between 1,150 and 1,250 °C, causing a fluctuation in the measured area. This effect explains why the cross-sectional area of the sample at 1,150 °C is practically the same as that at 1,200 °C (Fig. 5). This figure presents the mean of the values that were given in Fig. 4, allowing a better description of the general behavior of Vikaflex® during heating.

Figure 5 shows that in fact there is a general expansion step at temperatures up to 900 °C, after which a moderate shrinkage step occurs until 1,050 °C. Above this temperature, a significant dilation of the material occurs, which is evident from the significant increase in the projected areas (images D, E and F of Fig. 3). Because of this intense and irregular pyroexpansion above 1,050 °C, the thermal expansion coefficient was calculated only for temperatures up to 1,050 °C, in order to prevent significant measurement errors. The curves calculated from Eq. 1 up to 1,050 °C for each specimen are shown in Fig. 6.

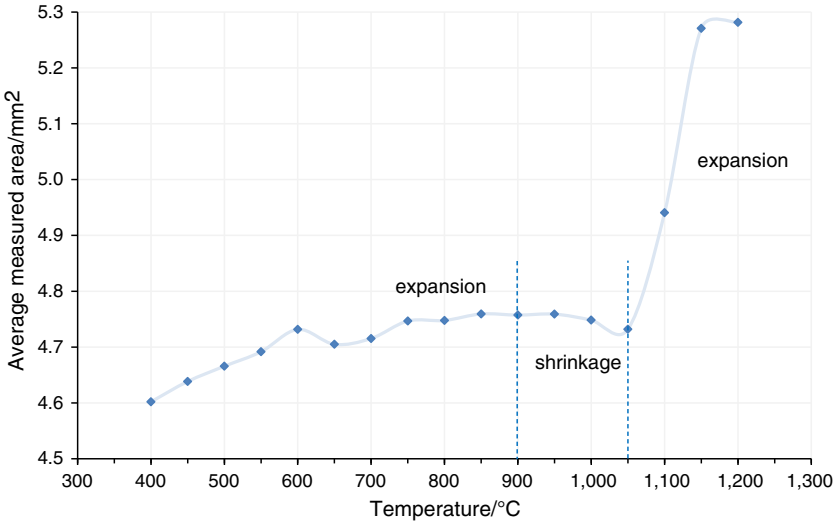

Fig. 5 Average cross-sectional area of three samples of Vikaflex as a function of temperature up to 1,200 °C

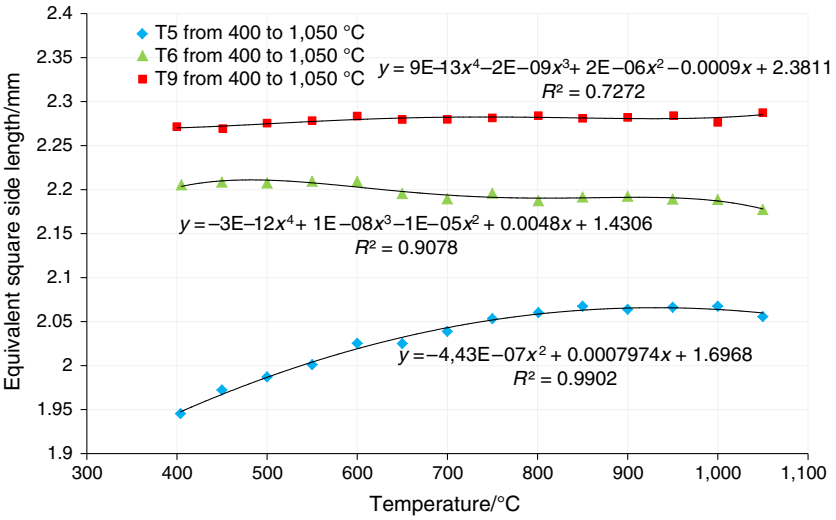

Fig. 6 Equivalent square side curves as a function of temperature for three different samples of Vikaflex at temperatures from 400 to 1,050 °C

From the curves depicting the variation of the length of the side of the equivalent square with temperature of the three samples shown in Fig. 6, respective linear thermal expansion coefficients were calculated for each sample as a function of temperature using Eq. 2. Then, the average values obtained for the samples, at each temperature considered, were calculated and plotted in Fig. 7. From the figure, it is possible to observe that calculated values show a maximum 0.000015 $°C^{-1}$ deviation from the fitted curve. This curve representing the average linear expansion coefficient as a function of temperature shows that Vikaflex® presents positive values of thermal expansion coefficient at temperatures above about 400 °C, but that progressively decreases as temperature increases, until they become negative at temperatures above about 900 °C. The inversion in the thermal linear expansion coefficient was observed in all tested samples at this temperature, when shrinkage due to the formation of liquid glassy phases occurs [40].

Shrinkage is characteristic during sintering of ceramic materials, being the macroscopic expression of the coalescence of solid precursor particles. In the present work, shrinkage was promoted by the formation of a liquid phase, with simultaneous elimination of pores. The sintering stage occurs from 900 to 1,050 °C, after which a disordered and intense structure expansion occurs up to 1,200 °C, as discussed earlier in the manuscript. As such, from 400 to 1,050 °C the mean linear expansion coefficient of Vikaflex® may be described by the polynomial:

$$\alpha = -7 \times 10^{-10} T^2 + 4 \times 10^{-7} T + 0.0002 \quad (3)$$

Thermal expansion values above 1,050 °C are much higher, as a result of the pyroexpansion promoted by thermal decompositions with gas generation. The

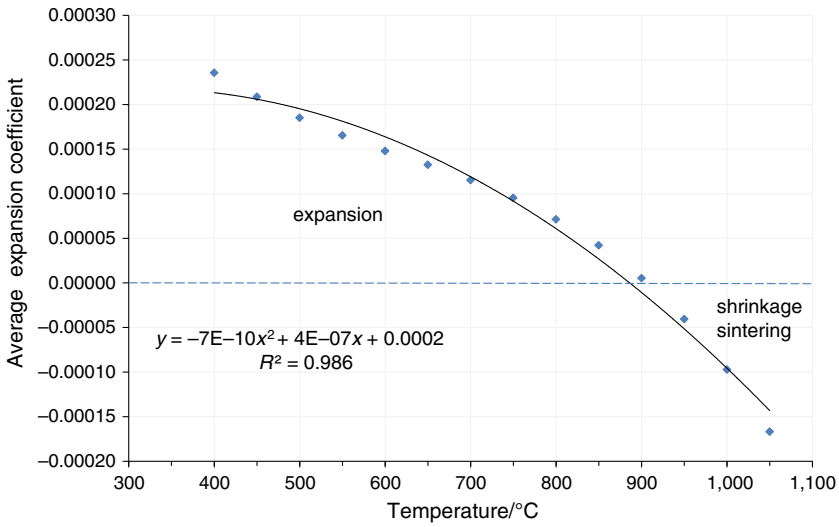

Fig. 7 Average linear thermal expansion coefficient of Vikaflex as a function of temperature from 400 to 1,050 °C

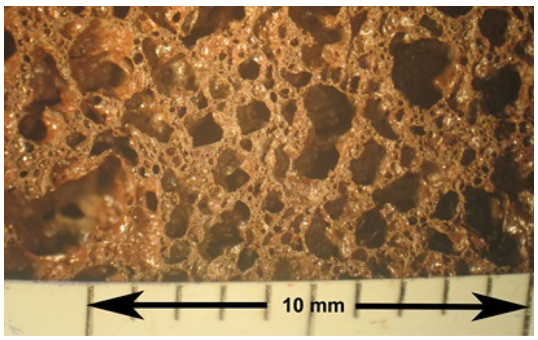

Fig. 8 Optical image showing the morphology of an internal surface of a Vikaflex® specimen at room temperature

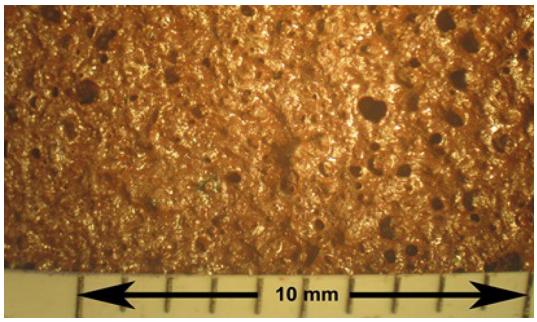

Fig. 9 Optical image showing the morphology of the external surface of Vikaflex® specimens at room temperature

generation of gases happens after the sintering stage, where a significant amount of liquid phase is also being formed, as can be seen in Fig. 8. Indeed, the figure shows the morphology of an internal surface cut at room temperature, with random closed pores that were identified by optical microscopy. This liquid phase keeps the gas inside the closed pores and tends to seal the outer surface of the pieces with a thicker glassy film, which were exposed to higher temperatures, as shown in Fig. 9, and also obtained at room temperature. The presence of an external surface with lower porosity is also evident from the figure, which shows some residual pores promoted by bubbles that are positioned higher up as they reach the surface, being expelled into the atmosphere of the oven.

After the sintering phase, the amount of free liquid phase among the non-melted phase particles increases significantly, creating a viscous layer that blocks the release of the gases formed by decomposition at higher temperatures. This film, flexible by its nature, allows the specimen to deform under the internal pressure of the gases. With heating reaching even higher temperatures, the liquid phase increases in volume, but its viscosity reduces, allowing not only the expansion of the pores where the gases are, but also mainly the decrease of the width of the external surface, allowing the gases to escape through it, causing subsequent collapse of the changing structure until its complete melting.

Although each sample presents slightly different behavior, this sequence occurs repeatedly, with inflections taking place at approximately the same temperature ranges. Thus, variations arise from differences in mass between the test samples, as well as those associated with the variability of the material produced in laboratory scale.

Thermal analysis

Interpretation of data from thermal analysis of Vikaflex® became more straightforward after understanding, from the test results presented up to this point, the effect of the increase in the proportion of vitreous and liquid glass phases on the thermal behavior of the sample. In order to better understand the glassy phase behavior, after the Vikaflex® sample was transformed in a liquid phase by

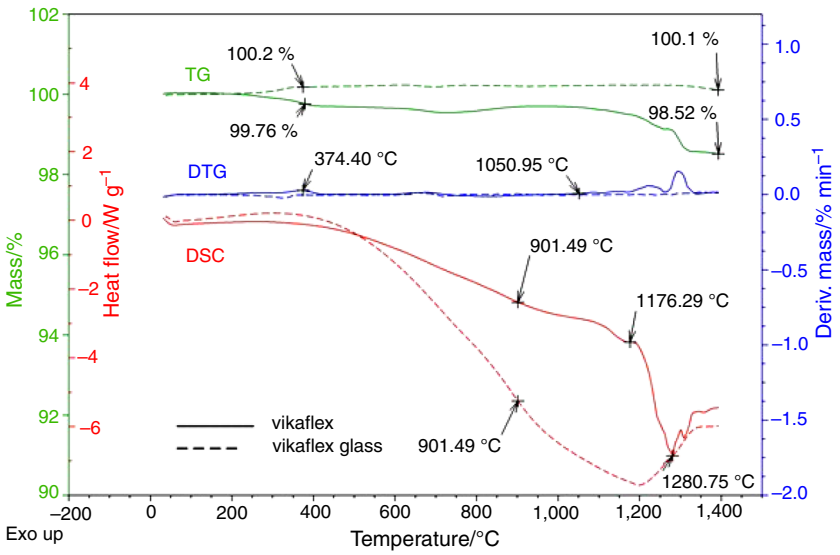

Fig. 10 TG, DTG and DSC curves of a Vikaflex® 2.5 × 2.5 × 2.5 mm cube and of the glass obtained from its melting

complete melting during its thermal analysis, it was cooled down to ambient temperature in the same crucible, resulting in a glass, which was immediately submitted to a new thermal analysis in air, up to 1,400 °C. TG, DTG and DSC curves of Vikaflex® and the glass obtained therefrom are presented in Fig. 10.

TG and DTG curves

The Vikaflex® TG curve (Fig. 10) presents, at first, very small mass loss (0.24 mass%) between 250 and 450 °C, as a result of the release of some previously trapped decomposable material in its closed pores. This mass loss is shown by the respective small DTG peak, with a maximum at 375 °C. Between the same temperature ranges, the TG curve of the glass sample shows a small gain in mass, possibly due to the completion of the oxidation of some ferrous oxide that is present. Above 400 °C, the TG curve of the glass is very stable, and the Vikaflex® TG curve remains stable up to 1,050 °C, when it shows a small mass loss, caused by the decomposition of some of its constituents. Depending on the temperature, the gas formed during this decomposition escapes from the pores where it is formed. As the increase of liquid phase decreases the pore stability, it causes its collapse as discussed previously. For instance, one of these constituents can be calcium sulfate, which was identified in the XRF analysis of the Vikaflex. Indeed, Marchal [41], in her study of $CaSO_4$ decomposition at elevated temperatures, reported that the presence of Fe_2O_3 promotes $CaSO_4$ decomposition by the following reaction:

$$CaSO_4 + Fe_2O_3 \rightarrow Fe_2O_3 \cdot CaO + SO_2 + 1/2\ O_2$$

Some of the gases that are promoting the pyroexpansion of Vikaflex may very possibly be sulfur dioxide and oxygen, which, in non-restricted environment, present total vapor pressure of 0.025 and 0.049 atm. at 1,040 and 1,097 °C, respectively. Additionally, the formed calcium ferrite (Fe_2O_3·CaO) melts at 1,250 °C [40], and given its high Fe_2O_3 content, partial melting of Vikaflex® begins at a lower temperature, resulting in the appearance of the softening point at 1,200 °C.

At 1,280 °C, the Vikaflex® TG curve presents an inflection, continuing to show loss of mass, but now in a higher rate as shown by the respective DTG peak (Fig. 10). This confirms the release of the formed gases from the outer more glassy and less viscous surface. Visible irregularities in the TG and DTG curves at the higher range of temperature after 1,200 °C are caused by the irregular escape of gases generated by thermal decompositions, as commented previously. The two samples are still losing mass at the end of the respective TG curves, showing that respective decompositions have not yet been completed at 1,380 °C.

DSC curves

DSC curves of Vikaflex® and its glass, shown in Fig. 10, present a broad slightly exothermic peak between 60 and 400 °C, which is more pronounced in the case of the glass. For the glass, as was seen in its TG curve, the oxidation of ferrous phase causes the exothermic effect. Very likely, same kind of ferrous to ferric oxidation is also occurring in the case of Vikaflex®, but as there is a small simultaneous mass loss, which is very probably endothermic, in its DSC curve only a very small exothermic effect may be identified.

Above 400 °C, the DSC curve of Vikaflex® shows an endothermic peak extending in a smooth curve during its softening until 1,175 °C. This curve has an inflection point at 900 °C, when the formation of liquid phase begins to

occur, promoting sintering of the material through the coalescence of particles and subsequent shrinkage of the sample. From 1,175 °C, the melting stage starts, identified by an intense endothermal peak until the 1,280 °C, when the need for heat to proceed melting begins to reduce, since most of the material is melted, and its viscosity is also reduced. At this temperature, there is also an increase in mass loss that is better identified from DTG peaks. After the end of melting DSC peak of Vikaflex®, one can identify the curve to stabilize, but at a lower base line, since the liquid material has a higher specific heat than the solid one, due to the poorer heat conductivity in a liquid medium.

Conclusions

Heating microscopy can be a useful technique for dimensional analysis, as well as for assisting in the understanding of changes in shape and phase transformations that occur as a function of temperature. The measurement of cross-sectional areas from images generated during heating microscopy allows a better evaluation of dimensional changes, enabling, in anisotropic conditions, the estimation of thermal expansion coefficients as a function of temperature.

Vikaflex® thermal expansion coefficient measurement from HM images indicated three different stages of dimensional change at the analyzed temperature range:

- In the first stage, the expansion coefficient is positive, but continuously decreasing in value up to 900 °C.
- As the temperature increases, a second phase occurs, when the thermal expansion coefficient becomes negative and increases in magnitude due to sintering effect promoted by the formation of a liquid phase.
- The third stage starts abruptly, when a decomposition step begins, forming gases that promote pyroexpansion, with an expansion behavior. This third stage begins with a high expansion rate, promoting an irregular foaming step, whose intensity decreases, as the proportion of liquid phase increases. During this stage, the higher the temperature, the lower the viscosity of the liquid phase and the higher the likelihood that the formed gases escape through the covering liquid phase. The result is that the product progressively loses stability, structure and size, until it melts completely.

The various thermal analyses indicate that Vikaflex® is a ceramic material fairly stable at temperatures of up to 1,050 °C, which can be used as a construction material.

Acknowledgements The authors would like to thank Centro de Tecnologia Mineral (CETEM), and in particular Dr. Reiner Newman, for assistance in the chemical analyses.

References

1. Raupp-Pereira F, Hotza D, Segadães AM, Labrincha JA. Ceramic formulations prepared with industrial wastes and natural subproducts. Ceram Intern. 2006;32:173–9.
2. Fonseca MVA. Vikaflex: um novo material cerâmico leve para a construção civil in Xisto—Pesquisas, Revisões e Ensaios Realizados no Brasil, Ed CRV. 2014:135–60.
3. Fonseca MVA. Reciclagem de rejeitos sólidos; desenvolvimento, em escala de laboratório, de materiais vítreos a partir do xisto retortado de S Mateus Sul, PR. Doc dissert, USP, SP, Br. 1990.
4. Q X, Li X, Li W, Zhou H, Xu S. Attapulgite-shale river bottom sludge ceramic particle sintered porous construction block, Faming Zhuanli Shenqing, CN 102924056 A 20130213. 2013.
5. Jin Y, Chen D. Oil shale residue aerated brick and manufacture method, Faming Zhuanli Shenqing, CN 102875184 A 20130116. 2013.
6. Weng L, Shale composite sintered brick for walling and its manufacture, Faming Zhuanli Shenqing, CN 101353250 A 20090128. 2009.
7. Colak M, Ozkan I. Sintering properties of the Bornova shale (Turkey) and its application in the production of red fired ceramics. Ind Ceram. 2011;31(3):209–15.
8. Shil'tsina AD, Selivanov VM. Non-plastic raw material for production of construction ceramics in Khakassia. Izvestiya Vysshikh Uchebnykh Zavedenii, Stroitel'stvo. 1998;2:53–6.
9. Hou Z, Mao X, Liu D. Method for manufacturing foamed ceramic heat-insulating plate from shale and clinker, Faming Zhuanli Shenqing, CN 103011786 A 20130403. 2013.
10. Jin J, Jin J. Method for preparation of high-performance ultralightweight foam ceramics with shale as main raw material, Faming Zhuanli Shenqing, CN 102603347 A 20120725. 2012.
11. Feng Z, Xue X, Li Y, Yang H. Preparation of foam glass-ceramic from oil shale residue. Guocheng Gongcheng Xuebao. 2008;8(2):378–83.
12. Li Y, Liu C. Foam glass prepared from shale, and its preparation method, Faming Zhuanli Shenqing, CN 103570245 A 20140212. 2014.
13. Takada T, Sarai H, Takahashi T, Miyazaki Y. Manufacture of bubble glass from shale, Jpn. Kokai Tokkyo Koho, JP 01141839 A 19890602. 1989.
14. Jin J, Jin J. Ultra-light vitreous foam ceramic and preparation method thereof by crushing, pelleting, screening, molding sintering and cutting, Faming Zhuanli Shenqing, CN 103922791 A 20140716. 2014.
15. Yang J, Chen J, Tang X, Qu X, Zhang P, Fan X, Xu L, Meng L, Tang Y, LVQ et al. Method for production of heat- and sound-insulating board, Faming Zhuanli Shenqing, CN 103803897 A 20140521. 2014.
16. Lu S, Yang L. Suspended shale ceramsite filtering material for water treatment and fabrication method, Faming Zhuanli Shenqing, CN 103304241 A 20130918. 2013.
17. Wang L. Wallboard and its manufacture method by resource utilization of municipal solid wastes, Faming Zhuanli Shenqing, CN 101239811 A 20080813. 2008.
18. Wu J, Zhu F, Xu X, Zeng Q, Chen J, Teng F. Method for production of environment-friendly water-permeable ceramic bricks, Faming Zhuanli Shenqing, CN 101328044 A 20081224. 2008.
19. Soares W, Menezes VJ, Fonseca MVA, Dweck J. Characterization of carbonaceous products by TG and DTA. J Therm Anal Calorim. 1997;49:657–61.
20. Perruso CR, Alcover Neto A, Neumann R, Nascimento RSV, Fonseca MVA. Powdered microporous glasses: changing porosity through aging. Cer Assoc Bras Ceram. 1998;44:289.

21. Getrouw MA, Fonseca MVA, Dutra AJB. Process for treatment of red mud for recovery of iron and aluminum hydroxides and production of glass ceramics, Brazil Pedido PI, BR 9602530 A 19981027. 1998.
22. Perruso CR, Alcover Neto A, Neumann R, Nunes RCR, Fonseca MVA, Nascimento RSV. Oil shale solid waste recycling in the development of new silica fillers for elastomeric composites. J Appl Polym Sci. 2001;81(12):56–2867.
23. Fonseca MVA. Process for fabrication of low-density ceramic product—lightweight board, Brazil Pedido PI, BR 2009002611 A2 20110412. 2011.
24. Dweck J, Morais LC, Fonseca MVA, Campos V, Büchler PM. Calcined sludge sintering evaluation by heating microscopy thermal analysis. J Therm Anal Calorim. 2009;95(3):985–9.
25. Aumond JJ, Scheibe LF. O fonolito de Lajes—SC, um novo fundente cerâmico brasileiro. Ceram Ind. 1996;1(2):17–21.
26. Arancibia JRH, Alfonso P, García-Valles M, Martínez S, Parcerisa D, Canet C, Romero YFM. Obtención de vidrio a partir de residuos de la minería del estaño en Bolivia. Bol Soc Esp de Cerám y Vidrio. 2013;52(3):143–50.
27. Venturelli C. Characterization of ceramic bodies through optical techniques: state of tension and green mechanical properties, suranaree. J Sci Technol. 2013;20(1):11–20.
28. Karamanov A, Dzhantov B, Paganelli M, Sighinolfi D. Glass transition temperature and activation energy of sintering by optical dilatometry. Thermoch Acta. 2013;553:1–7.
29. Sighinolfi D. Estudo experimental das deformações e estado de tensão em materiais cerâmicos tradicionais. Cerâm Ind. 2011;16(5–6):19–24.
30. Paganelli M, Venturelli C. The measurement of behaviour of ceramic materials during heat treatment. Process Eng. 2009;6:37–40.
31. DIN 51730:2007-09. Testing of solid fuels—determination of fusibility of fuel ash. http://www.beuth.de/en/standard/din-51730/98893895 (2014). Accessed 10 sept 2014.
32. Beveridge P, Doménech I, Pascual E, O Vidro—Técnicas de trabalho de forno; Ed Estampa, Lda, Lisboa. 2004.
33. Expert Solutions Advanced Thermal Analyses. Deformation temperature. http://www.expertsystemsolutions.com/search-and-documentation/glossary/d/deformation-temperature (2014) Accessed 15 Dec 2014.
34. Expert Solutions Advanced Thermal Analyses, Softening temperature. http://www.expertsystemsolutions.com/search-and-documentation/glossary/s/softening-temperature (2014). Accessed 15 Dec 2014.
35. Expert Solutions Advanced Thermal Analyses, Sphere temperature. http://www.expertsystemsolutions.com/search-and-documentation/glossary/h/hemisphere-temperature (2014). Accessed 15 Dec 2014.
36. Expert Solutions Advanced Thermal Analyses, Hemisphere temperature. http://www.expertsystemsolutions.com/search-and-documentation/glossary/h/hemisphere-temperature (2014). Accessed 15 Dec 2014.
37. Expert Solutions Advanced Thermal Analyses, Flow (Melting) temperature. http://www.expertsystemsolutions.com/search-and-documentation/glossary/f/flattening-melting-behaviour. Accessed 15 Dec 2014.
38. Callister WD. Fundamentals of materials science and engineering, an interactive E/text. 5th ed. NY, USA: Wiley; 2001.
39. Bagatini MC, Ghiggi MLF, Osório E, Vilela ACF, Cruz R, Defendi G. Estudo da fusibilidade das cinzas de carvões em função da composição química e mineralógica. Tec Metal e Mat. 2007;3(4):52–8.
40. Sousa JJF, Diehl LMA, Vugman NV, Fonseca MVA, Costa Neto C. Electron paramagnetic resonance and Moessbauer spectrometry of spent oil shale undergoing thermal treatment. An Acad Brasi Ciên. 1994;66(1):13–22.
41. Marchal G. Recherches sur la decomposition des sulfates metalliques par la chaleur. J Chem Phisiq. 1926;23:38–60.